Erythropoietin-directed erythropoiesis depends on serpin inhibition of erythroblast lysosomal cathepsins

Arvind Dev,[1] Susan M. Byrne,[2] Rakesh Verma,[1] Philip G. Ashton-Rickardt,[2] and Don M. Wojchowski[1]

[1]Center of Excellence in Stem Cell Biology and Regenerative Medicine (COBRE), Maine Medical Center Research Institute, Scarborough, ME 04074
[2]Section of Immunobiology, Division of Immunology and Inflammation, Department of Medicine, Faculty of Medicine, Imperial College London, SW7 2A7 London, England, UK

Erythropoietin (EPO) and its cell surface receptor (EPOR) are essential for red blood cell production and exert important cytoprotective effects on select vascular, immune, and cancer cells. To discover novel EPO action modes, we profiled the transcriptome of primary erythroid progenitors. We report *Serpina3g*/Spi2A as a major new EPO/EPOR target for the survival of erythroid progenitors. In knockout mice, loss of Spi2A worsened anemia caused by hemolysis, radiation, or transplantation. EPO-induced erythropoiesis also was compromised. In particular, maturing erythroblasts required Spi2A for cytoprotection, with iron and reactive oxygen species as cytotoxic agents. Spi2A defects were ameliorated by cathepsin-B/L inhibition, and by genetic co-deletion of lysosomal cathepsin B. Pharmacological inhibition of cathepsin B/L enhanced EPO-induced red cell formation in normal mice. Overall, we define an unexpected EPO action mode via an EPOR–Spi2A serpin–cathepsin axis in maturing erythroblasts, with lysosomal cathepsins as novel therapeutic targets.

CORRESPONDENCE
Don M. Wojchowski:
wojchd@mmc.org
OR
Philip G. Ashton-Rickardt:
p.ashton-rickardt@imperial.ac.uk

Abbreviations used: EPO, erythropoietin; EPOR, EPO receptor; EPC, erythroid progenitor cell; LMP, lysosome membrane permeability; PCD, programmed cell death.

In response to anemia, erythropoietin (EPO) is produced by renal interstitial fibroblasts (Asada et al., 2011). Within adult bone marrow, EPO then acts via its JAK2 kinase–coupled cell surface receptor (EPOR) to promote erythroid progenitor cell (EPC) formation (Wojchowski et al., 2010). Clinically, EPO is used to treat the anemia of chronic kidney disease (Del Vecchio et al., 2010) and, at restricted doses, the anemia caused by chemotherapy (Dicato and Plawny, 2010). However, EPO can also have an impact on innate immunity (Nairz et al., 2011), diabetes (Choi et al., 2010), vasculogenesis (Wojchowski et al., 2010), and the progression of certain cancers (Dicato and Plawny, 2010), and it exerts hypertensive and thrombolytic side-effects (Krapf and Hulter, 2009; Spivak et al., 2009). These observations, together with the clinical emergence of new EPOR agonists (DelVecchio et al., 2010) provide compelling reasons to better understand key EPO/EPOR actions. This includes effects on EPCs as a prime target in which EPO/EPOR actions remain incompletely understood. Canonical pathways involving PI3K and RAS/MEK/ERK, for example, are well studied (Wojchowski et al., 2010), but important new EPOR effectors continue to be uncovered. Recent examples include inhibition of NF-κB pathways in macrophage (Nairz et al., 2011); EPOR interactions with transferrin receptor 2 (Forejtnikovà et al., 2010); and IgA effects on EPOR signaling (Coulon et al., 2011). In this study, we report on a novel EPO/EPOR–serpin–lysosomal cathepsin axis that can sharply modulate the survival of maturing erythroblasts as an unexpected target for cytoprotection.

RESULTS AND DISCUSSION

We initially identified *Serpina3g* as an EPO/EPOR-regulated factor that could exert apparent prosurvival effects in a cell line model (Sathyanarayana et al., 2008). Global transcriptome analyses of EPO-modulated targets in primary CFUe-like progenitors (stage "E1") defined *Serpina3g* (the locus encoding Spi2A) to be

A. Dev and S.M. Byrne contributed equally to this paper.

The Rockefeller University Press $30.00
J. Exp. Med. 2013 Vol. 210 No. 2 225-232
www.jem.org/cgi/doi/10.1084/jem.20121762

The Journal of Experimental Medicine

induced at levels comparable to the known major EPO response genes *Oncostatin-M*, *Socs2*, *Irs2*, *Egr1*, and *Cyclin-d2* (Fig. 1 A; Fang et al., 2007; Croker et al., 2008; Sathyanarayana et al., 2008; Wojchowski et al., 2010). In developing proerythroblasts (stage E2), *Serpina3g* induction (among EPO/EPOR targets) was additionally heightened (Fig. 1 B). In these bone marrow EPCs, the previously implicated EPO response factors *Bcl-x*, *Bcl2*, and *Mcl1* (Socolovsky et al., 1999; Josefsen et al., 2000) were not significantly up-regulated. For *Serpina3g*, more than fourfold induction by EPO in ex vivo–expanded bone marrow EPCs was also confirmed via quantitative RT-PCR. In addition, analyses using bone marrow EPCs from mice harboring knocked-in EPOR-H or EPOR-HM alleles (Menon et al., 2006) implicated roles for EPOR/PY343/Stat5 signals in *Serpina3g* induction (unpublished data).

To investigate the role of Spi2A in erythropoiesis, the *Serpina3g* locus was disrupted, and Spi2A$^{-/-}$ mice were generated (Fig. 2, A–F; Supplemental materials and methods). At steady state, global Spi2A deletion did not significantly perturb hemoglobin, or peripheral blood cell levels (Table 1). CFUe or BFUe levels similarly were not altered, whereas renal *Epo* levels in Spi2A$^{-/-}$ mice were modestly elevated by more than twofold (unpublished data). When challenged by phenylhydrazine-induced hemolysis, however, Spi2A$^{-/-}$ mice exhibited substantially worsened anemia, with hematocrits of 28.3 ± 2.2% as compared with 39.2 ± 1.6% among WT controls (Fig. 2 G). Spi2A$^{-/-}$ spleen weights (day 6 after PHZ) were also lessened (119 ± 14 mg vs. 144 ± 18 mg for WT controls; $n = 6$; $P = 0.02$). In a model of short-term bone marrow transplantation, when Spi2A$^{-/-}$ donor cells were used to rescue the erythron of irradiated recipients, rebound hematocrits were limited to a mean of 32.2 ± 3.3% compared with 46.5 ± 2.5% as restored by transplanted WT donor cells (Fig. 2 H). After sublethal irradiation, rebound erythropoiesis also was selectively compromised because of Spi2A deletion (Fig. 2 I), whereas no significant effects on rebound lymphopoiesis were exhibited. Spi2A, as a major EPO/EPOR response factor, is therefore required for efficient stress erythropoiesis.

Possible effects of Spi2A deficiency on EPO-induced erythropoiesis were next studied. In Spi2A$^{-/-}$ mice, EPO-induced red cell formation was limited to 8.6 ± 0.7% of WT control levels (Fig. 3 A). Bone marrow–resident EPCs were therefore analyzed after EPO dosing, and Spi2A deficiency was revealed to compromise erythropoiesis at an erythroblast stage of development. This was most obvious among a resolved, relatively late-stage subpopulation of Ter119^{high} erythroblasts (designated stage E3.3; Fig. 3, B and C). This is consistent with EPO-induced accumulation of *Serpina3g* in developing EPCs, and functional deployment of Spi2A within stage E3 cells. Notably, Spi2A deficiency was specifically proven to compromise erythroblast survival (Fig. 3 D).

Why Spi2A deficiency has an impact on erythroblasts was studied next. During erythropoiesis, heme biosynthesis escalates, and developing erythroblasts exhibited sharp increases in levels of mRNA encoding *Alas2*, *Cpox*, and *Uros* heme-synthesizing enzymes, together with several iron transport factors (Fig. 4, A–C). In contrast, levels of the antioxidants *Sod2*, *Gadd45a*, and *Gstp* decreased. Heme generates an oxidative milieu (Fibach and Rachmilewitz, 2008), and we therefore intuited that Spi2A might confer cytoprotection against oxidative damage. This was tested by exposing primary erythroblasts to H_2O_2 (a physiological oxidant in erythroid cells; Friedman et al., 2004), and then measuring viability (Fig. 4 D). Frequencies of Spi2A$^{-/-}$ erythroblasts undergoing programmed cell death (PCD; YOPRO-3^{pos} cells) increased by 32.3% compared with 11.8% for WT erythroblasts after H_2O_2 exposure. In addition, Spi2A$^{-/-}$ erythroblasts exhibited heightened reactive oxygen species (ROS) levels upon peroxide exposure (Fig. 4 E). To extend this observation, Spi2A$^{-/-}$ or WT bone marrow was used to reconstitute the erythron in lethally irradiated recipients. Analyses of donor-derived splenic EPCs (14 d after transplant) revealed elevated ROS levels in Spi2A$^{-/-}$ erythroblasts, together with increased

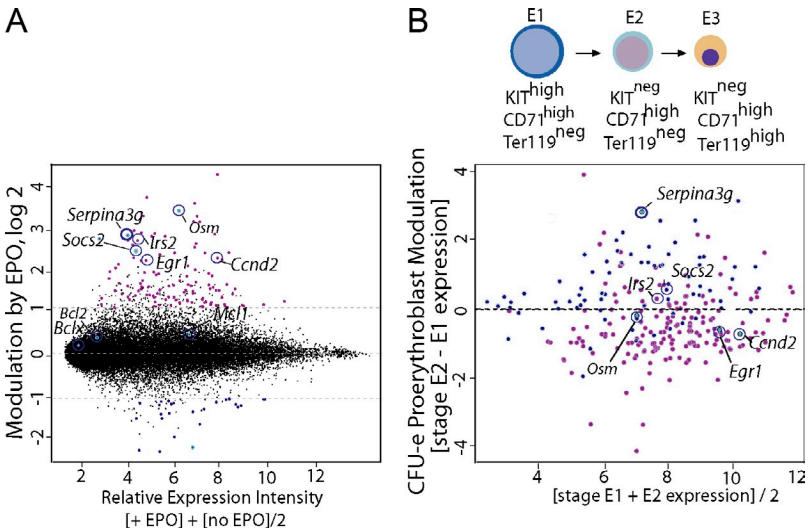

Figure 1. Global analyses of EPO-regulated genes in primary erythroid progenitors. (A) EPO-modulated transcripts in CFUe-like stage E1 cells were profiled (+/−EPO). All present calls are displayed based on relative expression intensity (x axis), with a logarithmic ordinate as fold-modulation by EPO. *Serpina3g* and the known EPO-response genes *Osm*, *Ccnd2*, *Socs2*, *Egr1*, and *Irs2* are annotated. (B) Substages E1–E3 of EPC development are outlined as CFUe-like cells, proerythroblasts, and erythroblasts (top). In stage E2 proerythroblasts, and among EPO-response genes, *Serpina3g* remains highly induced (bottom). This is based on relative expression levels for the 200 most modulated EPO-response genes (as compared with stage E2 vs. E1 cells). Findings in A and B derive from independent transcriptome experiments for E1 progenitors, and for E2 proerythroblasts.

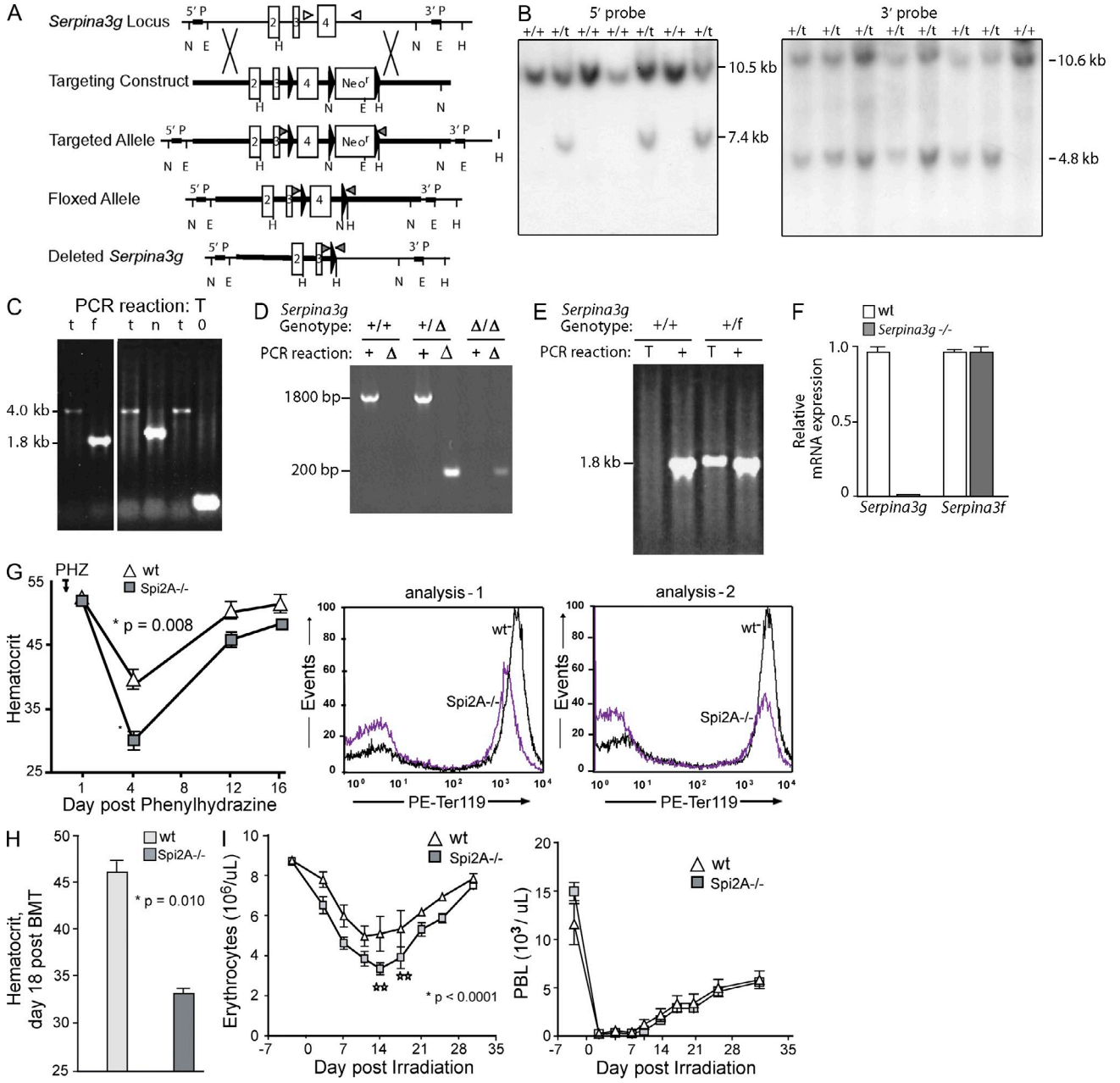

Figure 2. Spi2A deficiency worsens anemia. (A and B) Targeting of the *Serpina3g* locus and Southern blot analyses of ES cell clones harboring WT (+/+) or targeted (t) alleles. (see Supplemental materials and methods). (C) Cre recombination of targeted alleles to yield an exon-4–floxed allele. Transient expression of Cre recombinase in ES cells generated an exon-4 floxed allele (f, 1.8-kb PCR product; as well as nonrecombined targeted alleles as 4-kb products, and Neo^r cassette plus exon-4 doubly deleted alleles as 200-bp products; see Supplemental materials and methods). (D and E) Mice were genotyped using two sets of PCR primer pairs to ascertain germline transmission of the floxed *Serpina3g* allele. Mice possessing the floxed allele were then bred with transgenic EIIa-Cre mice to produce the deleted Spi2A$^{-/-}$ allele. Representative PCR results from a WT (+/+) and a heterozygous floxed (+/f) mouse are shown. (F) Loss of *Serpina3g* mRNA expression in Spi2A$^{-/-}$ splenocytes. As a control, mRNA from the adjacent *Serpina 3f* gene also was analyzed (in two independent experiments). (G) For Spi2A$^{-/-}$ mice and WT controls, hemolytic anemia was induced with phenylhydrazine (PHZ). Hematocrits (mean ± SE, n = 8) were determined at baseline, and the indicated intervals. Flow cytometry analyses of (pro)erythroblasts formed in spleen at d3 after PHZ dosing in Spi2A$^{-/-}$ and WT controls. Results are representative of two independent experiments. (H) Spi2A$^{-/-}$ donor cell reconstitution of the erythron. Irradiated recipients were transplanted with bone marrow from Spi2A$^{-/-}$ or WT mice. At d18 after transplant, hematocrits were determined (mean ± SE, n = 6). This effect of Spi2A deficiency on erythroid reconstitution has been consistently observed in three independent experiments. (I) After sublethal irradiation, hematopoiesis within Spi2A$^{-/-}$ mice within the erythroid lineage was analyzed. Mice were exposed to 7.5 Gy cesium-137. At the indicated time points, peripheral erythrocyte and leukocyte levels were assayed (mean ± SE, n = 5). Data are for a single independent experiment, but with full-design and 10 time-points analyzed.

Table 1. Hemoglobin, and peripheral blood cell levels in WT and Spi2A$^{-/-}$ mice

Genotype	RBCs	Hemoglobin	WBCs	Platelets	Lymphocytes	Monocytes	Eosinophils	Basophils
	$\times 10^6/\mu l$	g/dl	$\times 10^3/\mu l$	$\times 10^3/\mu l$	$\times 10^3/\mu l$	$\times 10^3/\mu l$	$\times 10^3/\mu l$	$\times 10^3/\mu l$
WT	10.16 ± 0.6	14.4 ± 0.3	7.72 ± 2.04	1,136 ± 232.74	6.42 ± 1.7	0.11 ± 0.03	0.29 ± 0.03	0.02 ± 0.01
Spi2A$^{-/-}$	9.90 ± 0.1	14.5 ± 0.1	7.88 ± 0.91	1,078 ± 248.45	5.04 ± 1.6	0.10 ± 0.01	0.37 ± 0.19	0.03 ± 0.01
P-value	0.40	0.87	0.86	0.68	0.18	0.51	0.40	0.04

frequencies of apoptosis (Fig. 4 F). As analyzed at day 8 after transplantation, Spi2A deficiency did not significantly affect levels of splenic stress BFUe (10.3 ± 2.4 compared with 8.8 ± 2.2 stress BFUe for WT and Spi2A$^{-/-}$ transplants, respectively). Maturing erythroid progenitors also actively sequester iron, and free iron can catalyze peroxidative events (Fibach and Rachmilewitz, 2010). Chelation of iron by desferrioxamine attenuated H_2O_2-induced erythroblast death in WT cells, and this effect was enhanced in Spi2A$^{-/-}$ erythroblasts (Fig. 4 G). These findings point to Spi2A-mediated cytoprotection of erythroblasts from iron/H_2O_2-mediated PCD.

Oxidative stress can induce lysosome membrane permeability (LMP), and the release of executioner cathepsins (Johansson et al., 2010). Cytoplasmic cathepsin B can induce PCD, and increase LMP by damaging mitochondria, which then release ROS (Repnik and Turk, 2010). When WT erythroblasts were exposed to peroxide, staining of the lysosomal marker Lamp1 was heightened because of apparently increased Lamp1 epitope exposure (Fig. 5 A), and thus was indicative of compromised lysosomal integrity. By direct comparison with WT erythroblasts, lysosomes within Spi2A$^{-/-}$ erythroblasts (in the absence of peroxide exposure) exhibited heightened Lamp1 staining (suggesting increased LMP). When exposed to peroxide, most Spi2A$^{-/-}$ erythroblasts were destroyed, whereas others exhibited high-level Lamp1 staining (Fig. 5 B). We next determined whether the effects of Spi2A deficiency on erythroblast lysosomes involved cathepsin-mediated PCD. Spi2A can directly inhibit lysosomal cysteine cathepsins, including executioner cathepsins B and L (Liu et al., 2003). In WT erythroblasts, the cathepsin B/L inhibitor

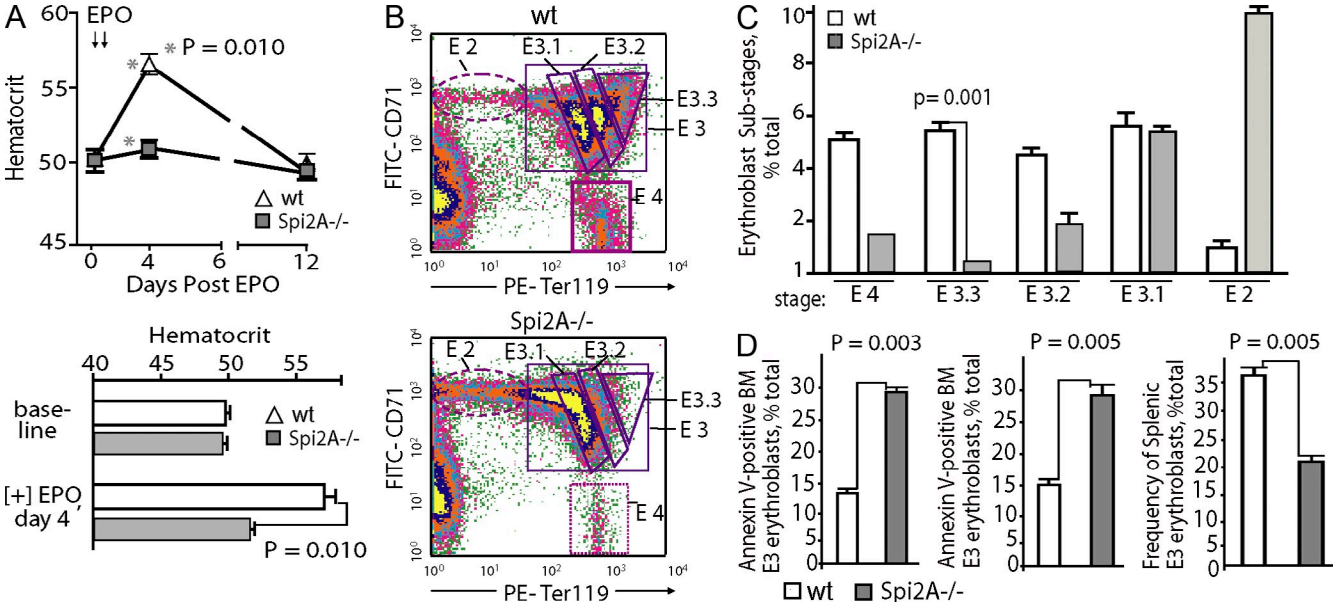

Figure 3. Spi2A is essential for efficient EPO-induced erythropoiesis, and its deletion compromises late-stage erythroblast formation. (A) Spi2A$^{-/-}$ and WT mice were challenged with EPO (1,250 U/kg at 1 and 24 h; arrows). At days 4 and 12 after EPO dosing (and at a 2-wk prior baseline mark), hematocrits were determined (top; mean ± SE, n = 5). Bottom panels illustrate repeated experiments (means ± SE, n = 8). These effects of Spi2A deficiency were observed in two independent experiments. (B and C) Spi2A$^{-/-}$ and control mice were challenged with EPO. 2 d later, frequencies of stage E2 proerythroblasts and stage E3 erythroblasts within bone marrow were determined (B). Based on graded increases in Ter119 expression during maturation, E3.1, E3.2, and E3.3 erythroblast subpopulations are gated. (C) Summary of observed frequencies of developing bone marrow proerythroblast cohorts (means ± SE, n = 3; as observed in two such analyses). (D, left) Frequencies of Annexin V–positive apoptotic Ter119^{pos} cells among bone marrow cells from EPO-dosed Spi2A$^{-/-}$ mice as compared to WT controls. (middle) As analyzed at day 3 after EPO-dosing, splenic erythroblasts from Spi2A$^{-/-}$ mice exhibited a 1.9-fold increase in frequencies of Annexin V–positive apoptotic Ter119^{pos} E3 cells as compared to WT controls. (right) EPO-induced erythroblast formation within spleen of EPO-dosed Spi2A$^{-/-}$ mice as 36.7% of splenocytes for EPO-dosed WT controls versus 22% for EPO-dosed Spi2A$^{-/-}$ mice (absolute numbers are 12.3 × 10^7 stage E3 cells among WT controls vs. 7.3 × 10^7 E3 cells among Spi2A$^{-/-}$ mice). Results in D were observed in two independent studies.

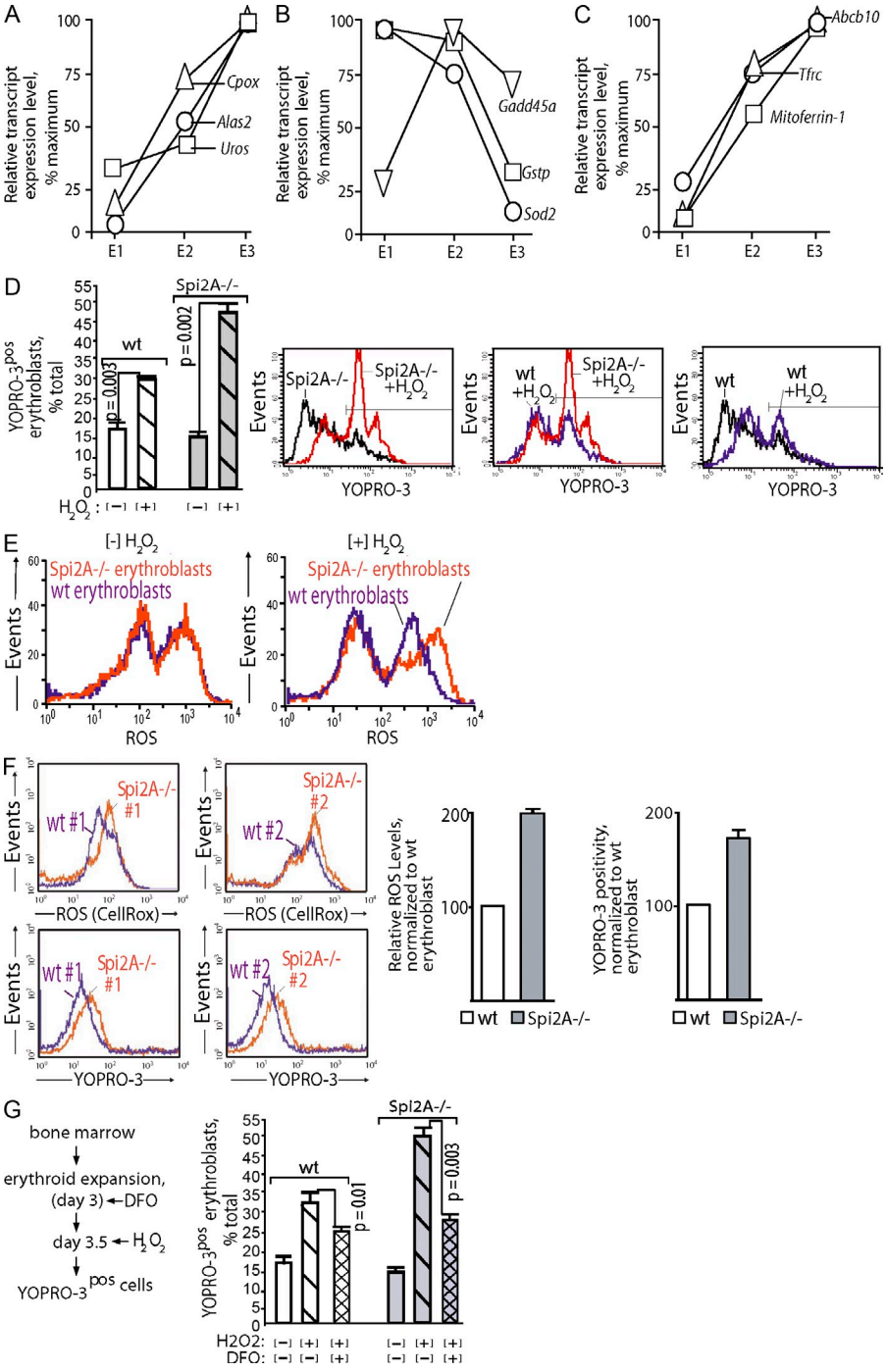

Figure 4. Spi2A$^{-/-}$ erythroblasts exhibit heightened sensitivity to oxidant-induced cell death. (A and B) In stage E3 erythroblasts, levels of heme biosynthetic enzymes increase, while levels of select antioxidant factors decrease: EPCs were expanded from WT bone marrow. CFUe, proerythroblasts, and erythroblasts (stage E1, 2, and 3 cells) were then purified and their transcript expression profiles were determined. In stage E3 erythroblasts, levels of several heme biosynthesis enzymes were substantially elevated including *Alas2*, *Cpox*, and *Uros*. In parallel, levels of the antioxidizing factors *Gstp*, *Sod2*, and *Gadd45a* decreased. (C) Stage E3 erythroblasts express elevated iron transport and iron metabolism factors. Transcriptome analyses of stage E1, E2, and E3 EPCs revealed heightened expression in erythroblasts of the *transferrin receptor*, *Abcb10*, and *Mitoferrin-1*. Data in A, is derived from independent full-design transcriptome analyses of isolated stage E1, E2, and E3 EPCs. (D) EPCs from WT and Spi2A$^{-/-}$ mice were expanded for 3.5 d (SP34ex medium). Cells then were exposed to H_2O_2 (4 h, 150 µM) and frequencies of nonviable erythroblasts were determined via YOPRO-3 staining of Ter119^{pos} cells. Summary data are graphed (means ± SE, $n = 4$) and representative primary flow cytometry data are shown. (E) ROS levels upon peroxide exposure: EPCs from WT and Spi2a$^{-/-}$ bone marrow were expanded, and Ter119^{pos} erythroblasts were isolated (by MACS). After exposure to peroxide (150 µM, 3 h) levels of ROS were determined by flow cytometry (Cell ROX). Findings in D and E are representative of two independent experiments. (F) ROS levels and apoptosis after bone marrow transplantation. Congenic Ly5.1 recipient mice were transplanted with WT or Spi2A$^{-/-}$ bone marrow cells. At day 16, levels of ROS in splenic erythroblasts were determined, together with levels of YOPRO-3–positive apoptotic erythroblasts. Representative primary flow cytometry data are shown (left) together with summary data for $n = 4$ mice (means ± SE). For differences in mean values for WT versus Spi2A$^{-/-}$ mice, p-values for ROS are: $P < 0.02$; and for YOPRO-3: $P < 0.02$. Results are for a single full-design experiment. (G) Iron chelation attenuation of H_2O_2-induced erythroblast death: EPC from bone marrow of WT or Spi2A$^{-/-}$ mice were expanded. On day 3 of culture, desferrioxamine (DFO) was added (±5 µM). On day 3.5, cells were challenged with H_2O_2, and frequencies of nonviable Ter119^{pos} erythroblasts were then determined. Values are means ± SE ($n = 3$). These effects have been observed in two separate analyses.

CA074Me (Buttle et al., 1992) conferred significant cytoprotection against peroxide-induced death (Fig. 5 C). In Spi2A$^{-/-}$ erythroblasts, cytoprotection by CA074Me was enhanced by up to 2.3-fold over WT effects. Thus, Spi2A protects erythroblasts from PCD by suppressing cathepsin B/L after ROS-induced LMP. A genetic approach also was applied to assess effects of the compound deletion of Spi2A plus lysosomal cathepsin B on EPO-induced red cell formation, and the severity of phenylhydrazine-induced anemia. Concomitant deletion of cathepsin B in Spi2A$^{-/-}$ x cathepsin B$^{-/-}$ mice (Deussing et al., 1998) partially rescued defects in EPO-induced red cell formation caused by Spi2A deletion. Specifically,

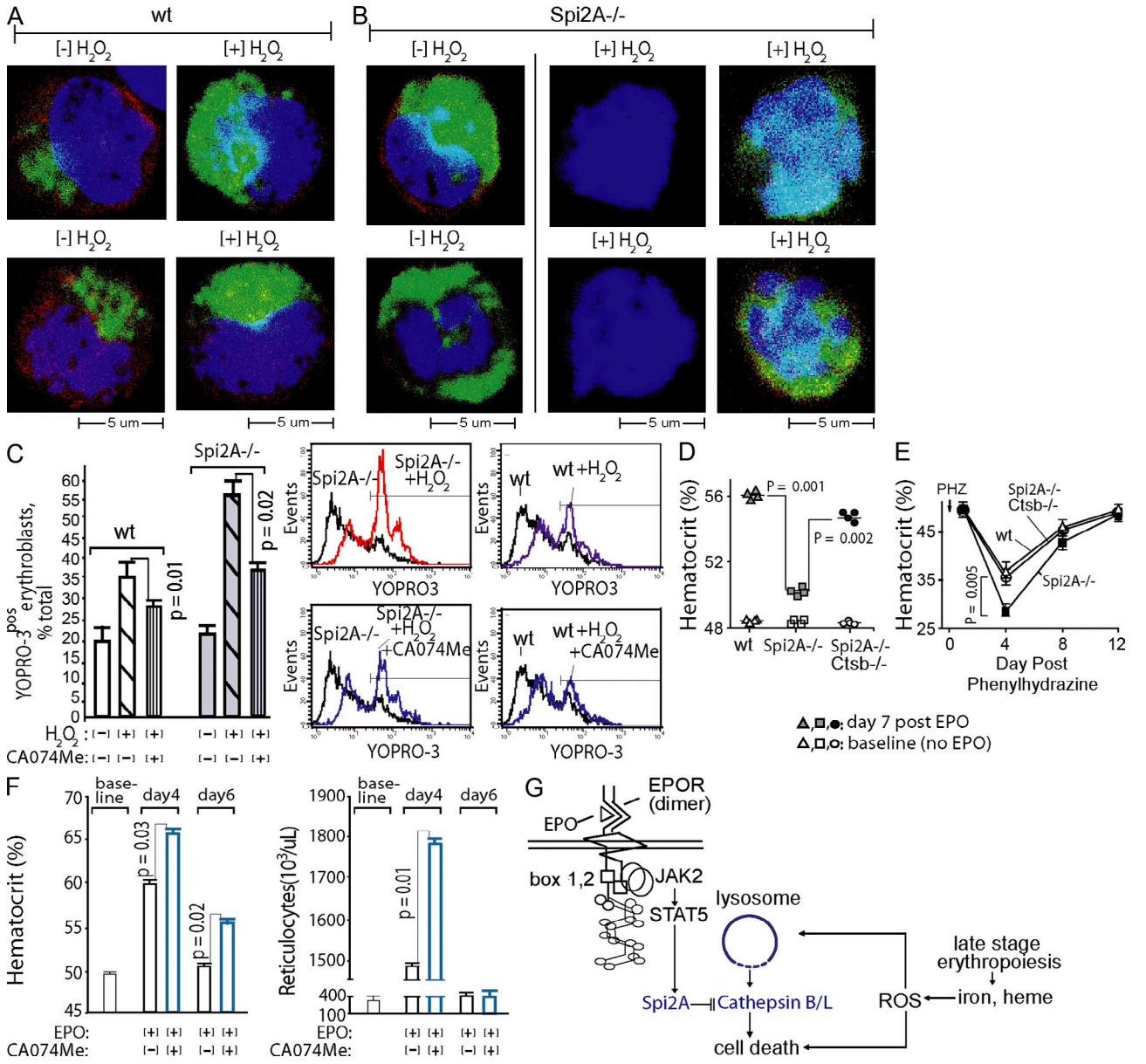

Figure 5. Adverse effects of Spi2A deficiency on erythropoiesis are diminished by lysosomal cathepsin B inhibition or deletion, and administration of CA074Me bolsters EPO-induced red cell formation in vivo. (A) Peroxide exposure enhances Lamp1 staining of lysosomes. When WT erythroblasts were examined for lysosome content via Lamp1 analysis, peroxide exposure proved to enhance Lamp1 staining (via apparent epitope unmasking). Images are representative of ≥10 acquisitions. (B) When Spi2A$^{-/-}$ erythroblasts were examined before peroxide exposure ([−] H_2O_2), Lamp1 staining was heightened (bottom left). Upon peroxide exposure, Spi2A$^{-/-}$ erythroblasts were largely destroyed, or exhibited further heightened Lamp1 staining of lysosomes (bottom right). Left and middle images are representative of ≥10 acquisitions. Compromised peroxide-exposed Spi2A$^{-/-}$ erythroblasts that remained intact (bottom right) were relatively less frequent (<10% of ruptured cells, which were detected largely as remnant nuclei; middle). (C) Erythroid progenitors were expanded from bone marrow of WT and Spi2A$^{-/-}$ mice. In subdivided cultures for each, either CA074Me (15 µM) or 0.1%DMSO (solvent control) was included. After 3 d, cells were challenged with H_2O_2 (150 µM, 4 h). CA074Me effects on erythroblast death then were determined (flow cytometry, YOPRO-3 staining among Ter119^{pos} cells). Data are mean values ± SE (n = 4). Representative primary flow cytometry data also are shown. Results are representative of three independent experiments. (D) WT, Spi2A$^{-/-}$, and Spi2A$^{-/-}$ x cathepsin B$^{-/-}$ mice were challenged with EPO (1,250 U/kg at 1 and 24 h). Levels of induced red cell production then were determined (mean hematocrits ± SE, n = 4). Baseline hematocrits (before EPO challenge) also are graphed. (E) For WT, Spi2A$^{-/-}$, and Spi2A$^{-/-}$ x cathepsin B$^{-/-}$ mice, hemolytic anemia was induced with phenylhydrazine (PHZ, 75 mg/kg). At the indicated intervals, hematocrits were then determined (means ± SE, n = 4). (F) WT mice were dosed with EPO (1,250 U/kg at 1 and 24 h), together with CA074Me (50 mg/kg, daily, see Materials and methods) or solvent control. At days 4 and 6 after EPO injection, levels of peripheral red blood cells (hematocrits) and reticulocytes were determined. Graphed values are means ± SE (n = 5 per treatment group). Findings in D–F are based on single full-design experiments. (G) A model is depicted in which EPO promotes erythroblast formation through *Serpina3g* induction, and Spi2A inhibition of lysosomal cathepsins B/L.

levels of red cell formation induced by EPO were restored to ~80% of WT levels (Fig. 5 D). In addition, the severity of hemolysis-induced anemia within Spi2A$^{-/-}$ mice was significantly lessened due to the compound deletion of cathepsin B (Fig. 5 E). Cathepsin B deficiency, per se, did not enhance EPO-induced red blood cell production (unpublished data), suggesting that protection from several executioner cysteine cathepsins may be required during EPO-induced erythropoiesis. Consistent with this interpretation, and of importance for clinical relevancy, CA074Me significantly ($P = 0.01$) enhanced EPO-induced red cell formation in WT mice (Fig. 5 F).

Collectively, our findings point to a novel mechanism for EPO cytoprotection in which the intracellular serpin Spi2A (as induced upon EPOR/JAK2 ligation) plays an integral role in EPO- and anemia-dependent erythropoiesis by inhibiting cathepsin B and/or L as lysosome-derived proteases (Fig. 5 G).

Within developing erythroblasts, we specifically suggest that ROS (Blomgran et al., 2007) as generated by iron and heme accumulation (Fibach and Rachmilewitz, 2010) brings about LMP and subsequent cell death through cathepsins. Lysosomal cysteine cathepsins may then stimulate mitochondrial pathways of PCD through the proteolytic activation of proapoptotic Bid (to p15t-Bid) and/or the degradation of the antiapoptotic factors Bcl2, Bcl_{XL}, and/or Mcl-1 (Johansson et al., 2010; Repnik and Turk, 2010). Damage to mitochondria also produces ROS, which can amplify LMP and subsequent PCD (Repnik and Turk, 2010). Therefore, Spi2A inhibition of cathepsin B may lie both upstream and downstream of ROS-induced LMP. Clinically, among predominant red cell disorders such as sickle cell anemia (George et al., 2010) and thalassemia (Fibach and Rachmilewitz, 2010), heightened ROS has been linked to oxidative stress and damage. Pharmacological inhibition of cathepsin B/L also mimicked the cytoprotective effects of EPO in vivo, and this finding points to new targets that determine rates of erythroblast production, and viability. Therefore, administration of small molecule inhibitors to cathepsin-B/L during anemia may act in erythroid cell–intrinsic ways to bolster red cell production. This could decrease effective EPO dosing levels; potentially lessen thrombolytic and hypertensive side-effects of EPO (Spivak et al., 2009; Krapf and Hulter, 2009); and, perhaps, benefit patients with chemotherapy-induced anemia for whom EPO dosing is now limited (because of potential effects on cancer progression; Spivak et al., 2009; Dicato and Plawny, 2010).

MATERIALS AND METHODS

Mouse lines and anemia models. Approaches used in the disruption of the *Serpina3g* locus in murine ES cells, and the generation of Spi2A$^{-/-}$ mice (plus Spi2A$^{-/-}$ x cathepsin B$^{-/-}$ mice) are described in Supplemental materials and methods, which also defines the anemia models used (phenylhydrazine-induced hemolysis, sublethal irradiation, 5-fluorouracil dosing, and bone marrow transplantation). Mouse maintenance and all procedures were approved by the University of Chicago, the Maine Medical Center Institutional Animal Care and Use Committee, and the UK Home Office.

Primary EPCs. For ex vivo analyses, primary EPCs were expanded from bone marrow preparations under optimized ex vivo culture conditions (Dev et al., 2010). Where specified, developmentally staged CFUe-like progenitors, proerythroblasts, and/or Ter119^{pos} erythroblasts were purified using optimized MACS-based depletion and selection procedures (Dev et al., 2010; Supplemental materials and methods).

Transcriptome analyses. Stage E1 CFU-e like EPC, and stage E2 proerythroblasts were expanded from WT EPOR mice, purified, and cultured for 6 h in IMDM, 0.5% BSA, holo-100 μg/ml transferrin, and 15 ng/ml insulin. Cells then were exposed to EPO (±4 U/ml) for 90 min. RNA was isolated directly, and was used (4 μg) to synthesize biotin-cRNA. Hybridizations were to Affymetrix 430-2.0 arrays (GeneChip Scanner 3000; GCOS software). Gene profiling results are posted at NCBI-GEO. Data analyses were via GeneSpring software (version 11.0.1). In RT-PCR, RNA was reverse-transcribed (1 μg) and cDNA was used in quantitative PCR as previously described (Dev et al., 2010). Primer pairs used (SABiosciences) included *Serpina3g* and *beta-Actin*.

Flow cytometry and confocal microscopy. For flow cytometry, 10^6 cells were collected, washed, and incubated at 4°C in PBS, 0.1% BSA plus rat IgG (1 μg) for 15 min (0.2 ml volume). Cells were then stained (40 min, 4°C) with 2 μg/ml APC-CD117, 5 μg/ml FITC-CD71, and 5 μg/ml PE-Ter119 (BD). PBS-washed cells then were analyzed (FACSCalibur; BD; CellQuest software). In analyses of apoptosis and cell death, APC-Annexin V binding assays were performed in 140 mM NaCl, 2.5 mM $CaCl_2$, and 10 mM Hepes, pH 7.4, for 30 min at 25°C. In YOPRO-3 assays, cells (10^6) were washed, and incubated (20 min, 4°C) in PBS, 0.1% BSA plus rat IgG (2 μg and 0.2 ml). Cells were then stained with 4 μg/ml FITC-Ter119 (BD; 30 min, 4°C) and with 1 μM YOPRO-3 (Invitrogen; 15 min, 4°C) and analyzed directly via flow cytometry. ROS levels were assayed using Cell ROX reagent (Invitrogen). In all flow cytometry experiments, equivalent numbers of gated events were analyzed. For details of confocal microscopy procedures, please see Supplemental material and methods.

Cathepsin inhibitor studies. In ex vivo studies, CA074Me (Enzo Life Sciences) was reconstituted in DMSO at 15 mM; diluted 10-fold in 37°C PBS upon use; filtered (0.2 μm); and included in EPC expansion cultures at 15 μM (in 0.1% DMSO). Control cultures received vehicle only (0.01 volume of 10% DMSO, PBS to yield 0.1% DMSO). For in vivo studies, CA074Me was prepared in DMSO initially at 350 mg/ml. At the time of injections, this stock was diluted in sterile PBS, 2% DMSO to 5 mg/ml. 0.2 ml per 20-g mouse weight was then was administered on 7 consecutive days (−2, −1, 0, +1, +2, +3, +4). Injections were i.p. on days −2, −1, 0, +1, and +4, and i.v. on days +2 and +3. EPO injections (1,250 U/kg, i.p.) were on day 0 (1 h) and day +1 (24 h).

Statistical considerations. For tests of significance between mean values (plus variance) of control versus single-treatment groups, a two-tailed Student's *t* test was used (alpha, 0.05). In array analyses of EPO-modulated genes, RMA-processed data were analyzed via FDR at a stringency of 0.05.

Online supplemental material. Additional details on the generation of Spi2A$^{-/-}$ mice, anemia models, and primary hematopoietic cell analyses are provided within Supplemental materials and methods. Online supplemental material is available at http://www.jem.org/cgi/content/full/jem.20121762/DC1.

We thank N. Liu, M. Zhang, Y. Wang, and L. Levine for assistance in developing Spi2A$^{-/-}$ mice, and L. Degenstein for blastocyst injections. The expert efforts by R. Asch, S. Su, and E. Jachimowicz in characterization of primary EPCs are also gratefully acknowledged. C57BL/6 ES cells were obtained from Primogenix, Inc.

Investigations were supported by National Institutes of Health (NIH) R01DK089439 (D. Wojchowski), R01AI04508 (P.G. Ashton-Rickardt), and grants from The Wellcome Trust and Cancer Research UK (P.G. Ashton-Rickardt). Additional support was provided by Maine Medical Center Research Institute (MMCRI) core facilities in Progenitor Cell Analysis, and Molecular Phenotyping (as supported by NIH 8P20GM103465; D. Wojchowski). The authors also thank MMCRI's Vascular Biology Center (NIH 8P30GM103392) for confocal microscopy core support, and the

University of Vermont Medical School Microarray Facility together with Dr. Aishwarya Narayanan (Strand Life Sciences) for assistance with Affymetrix array analyses.

The authors have no conflicting financial interests.

Submitted: 6 August 2012
Accepted: 17 December 2012

REFERENCES

Asada, N., M. Takase, J. Nakamura, A. Oguchi, M. Asada, N. Suzuki, K. Yamamura, N. Nagoshi, S. Shibata, T.N. Rao, et al. 2011. Dysfunction of fibroblasts of extrarenal origin underlies renal fibrosis and renal anemia in mice. *J. Clin. Invest.* 121:3981–3990. http://dx.doi.org/10.1172/JCI57301

Blomgran, R., L. Zheng, and O. Stendahl. 2007. Cathepsin-cleaved Bid promotes apoptosis in human neutrophils via oxidative stress-induced lysosomal membrane permeabilization. *J. Leukoc. Biol.* 81:1213–1223. http://dx.doi.org/10.1189/jlb.0506359

Buttle, D.J., M. Murata, C.G. Knight, and A.J. Barrett. 1992. CA074 methyl ester: a proinhibitor for intracellular cathepsin B. *Arch. Biochem. Biophys.* 299:377–380. http://dx.doi.org/10.1016/0003-9861(92)90290-D

Choi, D., S.A. Schroer, S.Y. Lu, L. Wang, X. Wu, Y. Liu, Y. Zhang, H.Y. Gaisano, K.U. Wagner, H. Wu, et al. 2010. Erythropoietin protects against diabetes through direct effects on pancreatic beta cells. *J. Exp. Med.* 207:2831–2842. http://dx.doi.org/10.1084/jem.20100665

Coulon, S., M. Dussiot, D. Grapton, T.T. Maciel, P.H. Wang, C. Callens, M.K. Tiwari, S. Agarwal, A. Fricot, J. Vandekerckhove, et al. 2011. Polymeric IgA1 controls erythroblast proliferation and accelerates erythropoiesis recovery in anemia. *Nat. Med.* 17:1456–1465. http://dx.doi.org/10.1038/nm.2462

Croker, B.A., H. Kiu, and S.E. Nicholson. 2008. SOCS regulation of the JAK/STAT signalling pathway. *Semin. Cell Dev. Biol.* 19:414–422. http://dx.doi.org/10.1016/j.semcdb.2008.07.010

Del Vecchio, L., A. Cavalli, B. Tucci, and F. Locatelli. 2010. Chronic kidney disease-associated anemia: new remedies. *Curr. Opin. Investig. Drugs.* 11:1030–1038.

Deussing, J., W. Roth, P. Saftig, C. Peters, H.L. Ploegh, and J.A. Villadangos. 1998. Cathepsins B and D are dispensable for major histocompatibility complex class II-mediated antigen presentation. *Proc. Natl. Acad. Sci. USA.* 95:4516–4521. http://dx.doi.org/10.1073/pnas.95.8.4516

Dev, A., J. Fang, P. Sathyanarayana, A. Pradeep, C. Emerson, and D.M. Wojchowski. 2010. During EPO or anemia challenge, erythroid progenitor cells transit through a selectively expandable proerythroblast pool. *Blood.* 116:5334–5346. http://dx.doi.org/10.1182/blood-2009-12-258947

Dicato, M., and L. Plawny. 2010. Erythropoietin in cancer patients: pros and cons. *Curr. Opin. Oncol.* 22:307–311. http://dx.doi.org/10.1097/CCO.0b013e32833aa9de

Fang, J., M. Menon, W. Kapelle, O. Bogacheva, O. Bogachev, E. Houde, S. Browne, P. Sathyanarayana, and D.M. Wojchowski. 2007. EPO modulation of cell-cycle regulatory genes, and cell division, in primary bone marrow erythroblasts. *Blood.* 110:2361–2370. http://dx.doi.org/10.1182/blood-2006-12-063503

Fibach, E., and E. Rachmilewitz. 2008. The role of oxidative stress in hemolytic anemia. *Curr. Mol. Med.* 8:609–619. http://dx.doi.org/10.2174/156652408786241384

Fibach, E., and E.A. Rachmilewitz. 2010. The role of antioxidants and iron chelators in the treatment of oxidative stress in thalassemia. *Ann. N.Y. Acad. Sci.* 1202:10–16. http://dx.doi.org/10.1111/j.1749-6632.2010.05577.x

Forejtnikovà, H., M. Vieillevoye, Y. Zermati, M. Lambert, R.M. Pellegrino, S. Guihard, M. Gaudry, C. Camaschella, C. Lacombe, A. Roetto, et al. 2010. Transferrin receptor 2 is a component of the erythropoietin receptor complex and is required for efficient erythropoiesis. *Blood.* 116:5357–5367. http://dx.doi.org/10.1182/blood-2010-04-281360

Friedman, J.S., M.F. Lopez, M.D. Fleming, A. Rivera, F.M. Martin, M.L. Welsh, A. Boyd, S.R. Doctrow, and S.J. Burakoff. 2004. SOD2-deficiency anemia: protein oxidation and altered protein expression reveal targets of damage, stress response, and antioxidant responsiveness. *Blood.* 104:2565–2573. http://dx.doi.org/10.1182/blood-2003-11-3858

George, A., S. Pushkaran, L. Li, X. An, Y. Zheng, N. Mohandas, C.H. Joiner, and T.A. Kalfa. 2010. Altered phosphorylation of cytoskeleton proteins in sickle red blood cells: the role of protein kinase C, Rac GTPases, and reactive oxygen species. *Blood Cells Mol. Dis.* 45:41–45. http://dx.doi.org/10.1016/j.bcmd.2010.02.006

Johansson, A.C., H. Appelqvist, C. Nilsson, K. Kågedal, K. Roberg, and K. Ollinger. 2010. Regulation of apoptosis-associated lysosomal membrane permeabilization. *Apoptosis.* 15:527–540. http://dx.doi.org/10.1007/s10495-009-0452-5

Josefsen, D., J.H. Myklebust, J. Lømo, M. Sioud, H.K. Blomhoff, and E.B. Smeland. 2000. Differential expression of bcl-2 homologs in human CD34(+) hematopoietic progenitor cells induced to differentiate into erythroid or granulocytic cells. *Stem Cells.* 18:261–272. http://dx.doi.org/10.1634/stemcells.18-4-261

Krapf, R., and H.N. Hulter. 2009. Arterial hypertension induced by erythropoietin and erythropoiesis-stimulating agents (ESA). *Clin. J. Am. Soc. Nephrol.* 4:470–480. http://dx.doi.org/10.2215/CJN.05040908

Liu, N., S.M. Raja, F. Zazzeroni, S.S. Metkar, R. Shah, M. Zhang, Y. Wang, D. Brömme, W.A. Russin, J.C. Lee, et al. 2003. NF-kappaB protects from the lysosomal pathway of cell death. *EMBO J.* 22:5313–5322. http://dx.doi.org/10.1093/emboj/cdg510

Menon, M.P., V. Karur, O. Bogacheva, O. Bogachev, B. Cuetara, and D.M. Wojchowski. 2006. Signals for stress erythropoiesis are integrated via an erythropoietin receptor-phosphotyrosine-343-Stat5 axis. *J. Clin. Invest.* 116:683–694. http://dx.doi.org/10.1172/JCI25227

Nairz, M., A. Schroll, A.R. Moschen, T. Sonnweber, M. Theurl, I. Theurl, N. Taub, C. Jamnig, D. Neurauter, L.A. Huber, et al. 2011. Erythropoietin contrastingly affects bacterial infection and experimental colitis by inhibiting nuclear factor-κB-inducible immune pathways. *Immunity.* 34:61–74. http://dx.doi.org/10.1016/j.immuni.2011.01.002

Repnik, U., and B. Turk. 2010. Lysosomal-mitochondrial cross-talk during cell death. *Mitochondrion.* 10:662–669. http://dx.doi.org/10.1016/j.mito.2010.07.008

Sathyanarayana, P., A. Dev, J. Fang, E. Houde, O. Bogacheva, O. Bogachev, M. Menon, S. Browne, A. Pradeep, C. Emerson, and D.M. Wojchowski. 2008. EPO receptor circuits for primary erythroblast survival. *Blood.* 111:5390–5399. http://dx.doi.org/10.1182/blood-2007-10-119743

Socolovsky, M., A.E. Fallon, S. Wang, C. Brugnara, and H.F. Lodish. 1999. Fetal anemia and apoptosis of red cell progenitors in Stat5a$^{-/-}$5b$^{-/-}$ mice: a direct role for Stat5 in Bcl-X(L) induction. *Cell.* 98:181–191. http://dx.doi.org/10.1016/S0092-8674(00)81013-2

Spivak, J.L., P. Gascón, and H. Ludwig. 2009. Anemia management in oncology and hematology. *Oncologist.* 14(Suppl 1):43–56. http://dx.doi.org/10.1634/theoncologist.2009-S1-43

Wojchowski, D.M., P. Sathyanarayana, and A. Dev. 2010. Erythropoietin receptor response circuits. *Curr. Opin. Hematol.* 17:169–176.